Response to the referee #1

Manuscript: **M. L. Pöhlker et al., Long-term observations of cloud condensation nuclei over the Amazon rain forest – Part 2: Variability and characteristics of biomass burning, long-range transport, and pristine rain forest aerosols**, ACP-2017-847)

We appreciate the comments by Referee #1, which have been considered carefully and helped to improve the quality of our manuscript. The referee's comments and our responses are outlined in detail below:

[1.1]   Referee comment: P4, section 1.2: Please provide additional information about how four cases are representative the typical CCN variability in the Amazon basin. For example, how many days are dominated by NP or BB condition?

Author Response: We agree with the referee. Please refer to our response to comment **[2.3]** of referee #2, where this aspect is discussed in detail.

[1.2]   Referee comment: P6, section 2.3, The definition of the near-pristine periods is a little bit weak. It seemed that it was only based on BC. Will other urban pollution tracer be considered?

Author Response: The definition and analysis of near-pristine and pristine states as ATTO has been revised very carefully. Please refer to our detailed response to comment **[2.2]** by referee #2.

[1.3]   Referee comment: P7, section 2.4: ATTO tower is 325 m tall. What is the uncertainty we expect from the BT analysis start height of 1000 m?

Author Response: We have conducted a sensitivity test and found that backward trajectory start heights at 200 m and 1000 m gave similar results. A corresponding statement can be found in Sect. 2.3:

> "A sensitivity test confirmed that starting heights of the BTs at 200 and 1000 m AGL gave similar results. Accordingly, the chosen start height at 1000 m appears to be a good representation of the origin of the boundary layer air masses at ATTO."

Details on the backward trajectory analysis can be found in C. Pöhlker et al. (2018), which has been submitted to ACP. This reference is cited several times throughout the text to clarify aspects of backward trajectory patterns and land use in the ATTO footprint region.

[1.4]   Referee comment: P13, line 5-10, What is the percentage of stable northeasterly wind direction for the periods in Figure 5a?

Author Response: According the backward trajectory analysis, the percentage of NE and ENE trajectories is ~70 % during the wet season (i.e., Feb to May). A corresponding statement has been added in Sect., 2.7:

> "The BTs from the northern hemisphere (i.e., NE and ENE BT clusters) account for ~70 % of all BTs during the wet season. Among these ~70 %, ~30 % can be attributed to the NE BT clusters."

[1.5]   Referee comment: Figure 5, 7 and 8, If possible, please do not overlap k(S, Da) with the size distribution plot. It is very hard to read the color map in k(S,Da).

Author Response: We modified the layout of the figures 5, 7, 8, and 9, trying to improve the readability (i.e., changing the shape and thickness of $\kappa(S,D_a)$ markers). However, we prefer to keep the overlaid kappa and size distribution representation since this layout emphasizes best the corresponding patterns in both data sets and their close agreement, which is an important aspect of the corresponding discussion. In general, we are aware that the time series figures 5, 7, 8, and 9 are rich in data and therefore rather complex. Accordingly, we implement these (and all other figures) in high resolution for the revised version of the manuscript, which allows to zoom into the pdf files electronically in order to explore the details of the figures.

[1.6]   Referee comment: P15, line 5-10, The results here are not well supported. Andreae et al. 2017 showed that the UT particles consist predominately of organic material for aerosol size larger than 90 nm. For aerosol less than 60 nm, AMS had a hard time to determine chemical composition with good sensitivity.

Author Response: It is true that the sensitivity of AMS measurements drops with decreasing particle size. However, we feel that our statement on the proposed organic composition of the Aitken mode under *PR* conditions is well supported by (i) our observation of relatively low kappa levels, which suggest the presence or organic material and (ii) the concept of upper tropospheric nucleation and growth of ultra-fine particles as proposed by Andreae et al., 2018, which allow the plausible assumption that the chemical composition of the ~60 nm and ~90 nm particle is not fundamentally different.

[1.7]   Referee comment: P16, section 3.5, The Saharan dust confirmed by EDX are larger than 1 micron. The CCN discussed in this section are in much smaller size range. It is confusing to classify the LRT influence as Saharan dust influence.

Author Response: The LRT plumes contain rather complex (internal) mixtures of African smoke, Saharan dust, and marine aerosols. We feel that the manuscripts is clear in stating that the LRT plumes not *only* contain Saharan dust but also further components such as sea salt, smoke etc. Examples can be found in Sect. 3.2:

> "These LRT plumes mostly comprise a complex mixture of Saharan dust, African biomass burning smoke, and marine aerosols from the transatlantic air passage (e.g., Talbot et al., 1990; Swap et al., 1992; Gläser et al., 2015)"

and Sect. 3.5:

> "The African *LRT* plumes that frequently impact the Amazon Basin during the wet season comprise a complex mixture of different aerosols components, including (i) a fraction of Saharan dust (mostly >1 µm), (ii) biomass burning aerosols from fires in West Africa (mostly in the accumulation mode), and (iii) marine aerosols from the plume's transatlantic passage (in coarse and accumulation modes) (Andreae et al., 1986; Talbot et al., 1990; Swap et al., 1992; Weinzierl et al., 2017)."

In fact, the referee is right that the Saharan dust component in the complex LRT plumes is likely not the key component that primarily influences the CCN population. Instead, the sea spray and African smoke components likely play a more important role in altering the $\kappa(S,D_a)$ and particle size distributions as they reach further into the relevant CCN size range. These aspects are discussed in detail in the manuscript.

A further aspect worth mentioning is that most of the dust particles are indeed >1 µm. However, a certain fraction has been found also <1 µm by Weinzierl et al. (2017) in the Caribbean region. These results show that a dust influence on the CCN population cannot be excluded completely. The reference to the study by Weinzierl et al. (2017) has been newly added to the manuscript. A study, which analyzes the size ranges of the dust, salt and smoke fractions in the LRT plumes at ATTO is currently being prepared. First results of this analysis show – similar to Weinzierl et al. (2017) – that certain dust contributions can also be found in the submicron size range and thus reach into the CCN relevant range discussed here.

[1.8] <u>Referee comment:</u> P18, line 23-24, from Table 3, except LRT case, the rest of cases all have reasonably good agreement between kp and k(0.11%). It is very stretching to state the LRT case is in a good agreement.

<u>Author Response:</u> In the corresponding statement we say that κ_p and $\kappa(0.11\%)$ "agree reasonably well", which we still regard as an appropriately careful wording. Evidently, large fractions of the LRT aerosols are not detected by the ACSM, which only measures non-refractory components. This instrumental limitation likely explains the relatively large difference between κ_p and $\kappa(0.11\%)$. This is stated as follows in the corresponding text section: "The remaining difference between κ_p and $\kappa(0.11 \%)$ can likely be explained by further refractory inorganics that were not covered by the ACSM."

[1.9] <u>Referee comment:</u> P19, section 31, authors said that ": : :correspond to a clear drop in aerosol hygroscopicity: : :". Please clarify the "drop", compared to what cases?

<u>Author Response:</u> Thanks for pointing out that this aspect lacks clarity. We modified the corresponding statement to:

> "At the same time, the presence of the pyrogenic aerosols correspond to a clear drop in aerosol hygroscopicity in both, the Aitken ($\Delta\kappa_{Ait} \approx$ -0.05) and accumulation modes ($\Delta\kappa_{Acc} \approx$ -0.1), relative to the conditions before and after the major *BB* plume (see overlay of $\kappa(S,D_a)$ size distributions and the dN/dlog$D$ contour plot in Fig. 8d)."

[1.10] <u>Referee comment:</u> P22, line 37, what is the OA/SO4 ratio for LRT pollution periods in Figure 7? Are they consistent with this case, around 3?

<u>Author Response:</u> The OA/SO_4^{2-} ratios of the *LRT* and *MPOL* case studies are not consistent (see corresponding results in Table 3). Actually, they should not be consistent since the wet season LRT plumes and the LRT influence during the *MPOL* period in the dry season transport rather different aerosol mixtures. However, we are aware that using the abbreviation LRT in both contexts tends to be confusing. Accordingly, we revised the corresponding sections in the text to clarify that the wet season LRT influence is typically quite different from the dry season LRT influence.

[1.11] <u>Referee comment:</u> Figure 10, the different shape of the CCN efficiency spectra may related to the mixing state of aerosols for each case. It will be interesting to include that discussion.

<u>Author Response:</u> That is correct. The mixing state of the aerosol has an influence on the shape of the CCN efficiency spectra. To clarify this aspect, the following statement has been added to Sect. 3.9:

> "Their shape is influenced by (i) the shape of the N_{CN} size distribution (i.e., relative strength of Aitken vs. accumulation modes), (ii) the aerosol composition through the $\kappa(S,D_a)$ values and its

size dependence as well as (iii) the mixing state of the aerosol as represented in the κ and $N_{\mathrm{CN}}\,\kappa$ distributions."

To what extent the mixing state defines the shape of the spectra cannot be answered easily and requires an in-depth analysis. We agree with the referee's suggestion that the mixing state of the aerosol population has not been adequately addressed in the manuscript yet. Therefore, we conducted a thorough analysis of the aerosol mixing state with the help of the hygroscopicity distribution concept introduced by Su et al. (2010). Since this analysis provides interesting additional insights into the properties of the contrasting CCN conditions, we decided to include a new figure (i.e., Fig. 10 in the revised version) and new dedicated text paragraph (Sect. 3.8 in the revised version) into the manuscript to discuss the relevant aspects as follows:

"3.8 Aerosol particle hygroscopicity distributions and aerosol mixing state

In this section, we investigate the aerosol particle mixing state for the different case study conditions with the help of the aerosol particle hygroscopicity distribution – or κ distribution – concept introduced by Su et al. (2010). This approach visualizes the spread of κ values among particles of a given size. Specifically, in an ideal internal particle mixture, all particles have the same chemical composition and therefore the same hygroscopicity, resulting in a narrow and defined κ distribution. In an external mixture, the particles at a given size can have widely different chemical compositions and hygroscopicities, resulting in a broad κ distribution.

Figure 10 summarizes two versions of κ distributions for the contrasting case study conditions: (i) the 'classical' κ distributions according to Su et al. (2010), which emphasize the spread of κ levels for all particle diameters across the measured size range, and (ii) κ distributions weighted with the corresponding average particle size distributions from Fig. 6, which provide a quantitative overview of particle abundance as a function of hygroscopicity and size ($N_{\mathrm{CN}}\,\kappa$ distribution). The comparison of the κ and $N_{\mathrm{CN}}\,\kappa$ distributions for the contrasting case study conditions emphasizes similarities and differences between the corresponding aerosol populations, which allows drawing conclusions on the aerosol mixing state and microphysical properties.

The κ distributions for most conditions reflect a bimodal character of the corresponding aerosol distributions with distinctly different properties in the Aitken and accumulation modes as outlined in the discussion of Fig. 6. Specifically, all distributions show an increasing spread of κ levels towards larger particle diameters, which suggests a higher degree of external particle mixing and therefore a higher diversity of particle properties (i.e., hygroscopicity) in the accumulation than in the Aitken mode. As an example, the *BB* and *MPOL-BB* cases show a κ spread in the accumulation mode range that reaches from values well below 0.1 up to levels of about 1. Remarkably, the *PR* κ distribution differs from all other cases since it shows overall the smallest spread of κ over the entire size range. This suggests the Aitken and accumulation mode particles under *PR* conditions are two distinct and chemically rather homogeneous aerosol populations with a comparatively high degree of internal mixing. As an example, the *PR* Aitken mode particle population cover a defined κ range between ~0.1 and ~0.15. In contrast, the *LRT*, *BB*, and *MPOL* aerosol populations appear to be more externally mixed.

In addition to the diversity of the hygroscopicity as visible in the κ distributions, the $N_{\mathrm{CN}}\,\kappa$ distributions further emphasize the quantitative abundance of particles in the hygroscopicity-size space. Accordingly, the $N_{\mathrm{CN}}\,\kappa$ distributions can be regarded as signature-like representations of the aerosol microphysical state under certain conditions. Note that the $N_{\mathrm{CN}}\,\kappa$ distributions in Fig. 10 differ substantially from each other. The *PR* case shows a unique signature. The *LRT* and *MPOL-LRT* cases show certain similarities due to the fact that both are characterized by similar aerosol size distributions and comparatively high κ levels. The comparison of the relatively fresh *MPOL-BB* smoke and the relatively aged *BB* smoke emphasizes the aging-related increases in particle size and hygroscopicity by means of a characteristic shift of the dominant mode in the $N_{\mathrm{CN}}\,\kappa$ distributions. In both cases the spread of κ is rather large, indicating a comparatively strong external mixing in the smoke plumes. In essence, the κ distributions and $N_{\mathrm{CN}}\,\kappa$ distributions represent valuable overview representations, which combine characteristic

aerosol properties in terms of particle size, particle concentration, κ diversity, and aerosol mixing state in a fingerprint-like manner. So far, only very few studies (e.g., Mahish et al., 2018) have used the κ distribution or related concepts to characterize ambient aerosol properties. In the light of the results in Fig. 10, we suggest that this concept should be used more broadly as it provides valuable insights into the particle mixing state beyond the more established characterizations of aerosol and CCN properties."

The following Fig. 10 has been added to the manuscript:
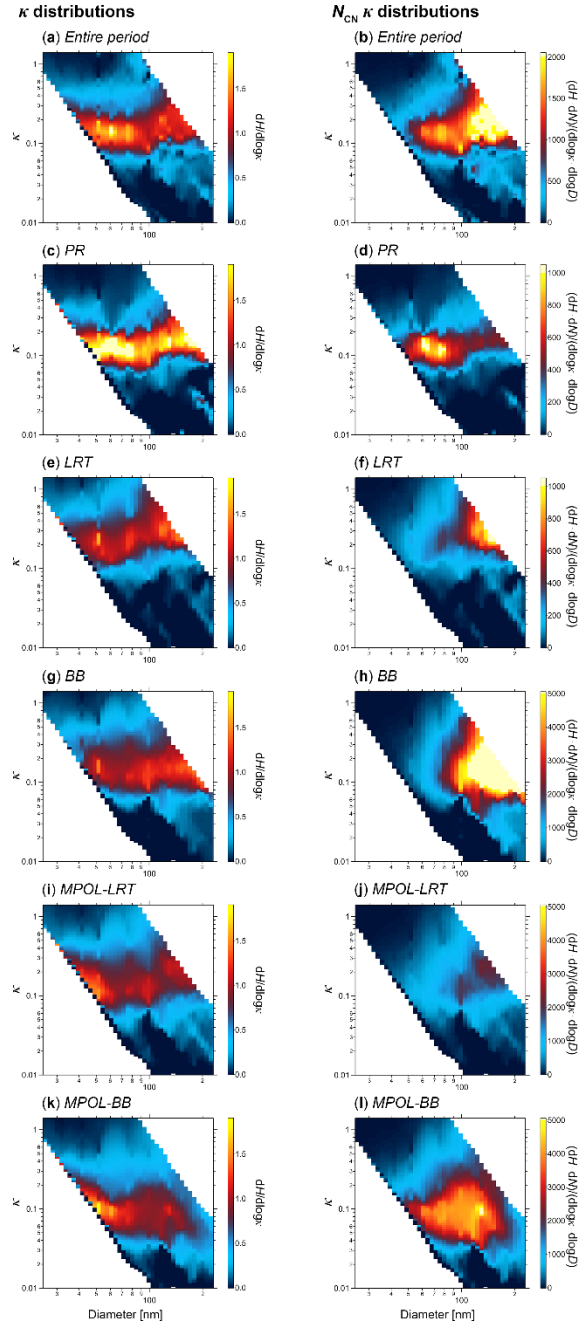
Figure 10. Average probability distribution of particle hygroscopicity, dH/dlogκ, on the left side and the same quantity weighted by the particle number size distribution, (dH·dN)/(dlogκ·dlog$D$), on the right side, plotted over the effective hygroscopicity parameter, κ, and dry particle diameter, D, for (a and b) the entire measurement period as well as (c and d) *PR*, (e and f) *LRT*, (g and h) *BB*, (i and j) *MPOL-LRT*, and (k and l) *MPOL-BB* conditions. The particle size distributions used for the weighting are shown in Fig. 6.

Moreover, the following concluding statement has been placed in the summary and conclusions section:

"Hygroscopicity distributions were analyzed for all conditions, providing detailed and characteristic insights into the mixing state of the different types of aerosols. We found that the spread of κ increases with size for all conditions. The κ distributions suggest that the *PR* aerosol population is rather internally mixed, whereas the *BB*, *LRT*, and *MPOL* aerosols show more external mixing states. In essence, the κ distributions and $N_{CN}\,\kappa$ distributions represent valuable overview representations, combining characteristic aerosol properties in terms of particle size, particle concentration, κ levels, and aerosol mixing state in a fingerprint-like manner. This representation helps to further understand aerosol-cloud interactions, such as the shapes of the CCN efficiency spectra: As general tendencies, more externally mixed aerosols, resulting in broader κ distributions, also broaden the CCN efficiency spectra – analogous to broad N_{CN} distributions. Internally mixed aerosols with more defined κ distributions tend towards steeper segments in the CCN efficiency spectra. Furthermore, externally mixed aerosols with distinctly different κ levels tend to introduce further steps/plateaus into the CCN efficiency spectra, in addition to plateaus caused by multimodal N_{CN} distributions. However, the CCN efficiency spectra for the conditions reported here are primarily shaped by the particle size distributions and average κ levels, whereas the diversity of κ seems to play a minor role. To clarify exactly how the signatures and patterns in κ and $N_{CN}\,\kappa$ distributions are related to the signatures and shapes of the CCN efficiency spectra, dedicated future studies at contrasting locations and modelling support is required."

References

Andreae, M. O., Afchine, A., Albrecht, R., Holanda, B. A., Artaxo, P., Barbosa, H. M. J., Borrmann, S., Cecchini, M. A., Costa, A., Dollner, M., Fütterer, D., Järvinen, E., Jurkat, T., Klimach, T., Konemann, T., Knote, C., Krämer, M., Krisna, T., Machado, L. A. T., Mertes, S., Minikin, A., Pöhlker, C., Pöhlker, M. L., Pöschl, U., Rosenfeld, D., Sauer, D., Schlager, H., Schnaiter, M., Schneider, J., Schulz, C., Spanu, A., Sperling, V. B., Voigt, C., Walser, A., Wang, J., Weinzierl, B., Wendisch, M., and Ziereis, H.: Aerosol characteristics and particle production in the upper troposphere over the Amazon Basin, Atmos. Chem. Phys., 18, 921-961, 10.5194/acp-18-921-2018, 2018.

Andreae, M. O., Charlson, R. J., Bruynseels, F., Storms, H., Vangrieken, R., and Maenhaut, W.: Internal Mixture of Sea Salt, Silicates, and Excess Sulfate in Marine Aerosols, Science, 232, 1620-1623, 10.1126/science.232.4758.1620, 1986.

Gläser, G., Wernli, H., Kerkweg, A., and Teubler, F.: The transatlantic dust transport from North Africa to the Americas-Its characteristics and source regions, Journal of Geophysical Research-Atmospheres, 120, 11231-11252, 10.1002/2015jd023792, 2015.

Mahish, M., Jefferson, A., and Collins, D.: Influence of Common Assumptions Regarding Aerosol Composition and Mixing State on Predicted CCN Concentration, Atmosphere, 9, 54, 2018.

Pöhlker, C., Walter, D., Paulsen, H., Könemann, T., Rodríguez-Caballero, E., Moran-Zuloaga, D., Brito, J., Carbone, S., Degrendele, C., Després, V. R., Ditas, F., Holanda, B. A., Kaiser, J. W., Lammel, G., Lavrič, J. V., Jing, M., Pickersgill, D., Pöhlker, M. L., Praß, M., Ruckteschler, N., Saturno, J., Sörgel, M., Wang, Q., Weber, B., Wolff, S., Artaxo, P., Pöschl, U., and Andreae, M. O.: Land cover and its transformation in the backward trajectory footprint of the Amazon Tall Tower Observatory, Atmos. Chem. Phys. Diss, submitted, 2018.

Su, H., Rose, D., Cheng, Y. F., Gunthe, S. S., Massling, A., Stock, M., Wiedensohler, A., Andreae, M. O., and Poeschl, U.: Hygroscopicity distribution concept for measurement data analysis and modeling of aerosol particle mixing state with regard to hygroscopic growth and CCN activation, Atmospheric Chemistry and Physics, 10, 7489-7503, 10.5194/acp-10-7489-2010, 2010.

Swap, R., Garstang, M., Greco, S., Talbot, R., and Kallberg, P.: Saharan dust in the Amazon Basin, Tellus Series B-Chemical and Physical Meteorology, 44, 133-149, 10.1034/j.1600-0889.1992.t01-1-00005.x, 1992.

Talbot, R. W., Andreae, M. O., Berresheim, H., Artaxo, P., Garstang, M., Harriss, R. C., Beecher, K. M., and Li, S. M.: Aerosol chemsitry during the wet season in central Amazonian – The influence of long-range transport, Journal of Geophysical Research-Atmospheres, 95, 16955-16969, 10.1029/JD095iD10p16955, 1990.

Weinzierl, B., Ansmann, A., Prospero, J. M., Althausen, D., Benker, N., Chouza, F., Dollner, M., Farrell, D., Fomba, W. K., Freudenthaler, V., Gasteiger, J., Groß, S., Haarig, M., Heinold, B., Kandler, K., Kristensen, T. B., Mayol-Bracero, O. L., Müller, T., Reitebuch, O., Sauer, D., Schäfler, A., Schepanski, K., Spanu, A., Tegen, I., Toledano, C., and Walser, A.: The Saharan Aerosol Long-Range Transport and Aerosol–Cloud-Interaction Experiment: Overview and Selected Highlights, Bulletin of the American Meteorological Society, 98, 1427-1451, 10.1175/bams-d-15-00142.1, 2017.